LA-UR-83-999

(1) CONF-830606--6

Los Alamos National Laboratory is operated by the University of California for the United States Department of Energy under contract W 7405-ENG-36.

LA-UR--83-999

DE83 011110

TITLE: A CIRCUIT MODEL FOR THE EXPLOSIVE-DRIVEN PLATE GENERATOR

AUTHOR(S): R. S. Caird, M-6
D. Erickson, M-6
C. M. Fowler, M-6
B. L. Freeman, M-6
J. H. Goforth, M-6

SUBMITTED TO: Will be submitted for presentation at Third International Conference on Megagauss Magnetic Field Generation and Related Topics, 13-17 June 1983, Novosibirsk, USSR.

DISCLAIMER

This report was prepared as an account of work sponsored by an agency of the United States Government. Neither the United States Government nor any agency thereof, nor any of their employees, makes any warranty, express or implied, or assumes any legal liability or responsibility for the accuracy, completeness, or usefulness of any information, apparatus, product, or process disclosed, or represents that its use would not infringe privately owned rights. Reference herein to any specific commercial product, process, or service by trade name, trademark, manufacturer, or otherwise does not necessarily constitute or imply its endorsement, recommendation, or favoring by the United States Government or any agency thereof. The views and opinions of authors expressed herein do not necessarily state or reflect those of the United States Government or any agency thereof.

By acceptance of this article, the publisher recognizes that the U S Government retains a nonexclusive, royalty-free license to publish or reproduce the published form of this contribution or to allow others to do so, for U S Government purposes

The Los Alamos National Laboratory requests that the publisher identify this article as work performed under the auspices of the U S Department of Energy

MASTER

DISTRIBUTION OF THIS DOCUMENT IS UNLIMITED

Los Alamos National Laboratory
Los Alamos, New Mexico 87545

FORM NO 836 R4
ST NO 2629 5/81

A CIRCUIT MODEL FOR THE EXPLOSIVE-DRIVEN PLATE GENERATOR*

R. S. CAIRD, D. J. ERICKSON, C. M. FOWLER, B. L. FREEMAN AND J. H. GOFORTH
Los Alamos National Laboratory, Los Alamos, New Mexico 87545, U.S.A.

ABSTRACT. It is useful to model explosive-driven generators as lumped-parameter circuit elements in order to estimate performance in new applications and to optimize the design of experiments. The plate generator is essentially a parallel or tilted-plate transmission line in which the current-carrying flat-plate conductors are driven by plane-wave explosive systems. We have developed a simple model for the time-varying inductance of this system. First, an analytic expression is used to predict the plate motion. Then, the inductance is expressed as a function of plate separation to give the computational model. Time-dependent flux losses are accounted for by an increasing waste inductance. Model predictions are compared with the available shot data.

---

* Work supported by the United States Department of Energy.

1. INTRODUCTION

The explosive-driven plate generator has been described in several previous publications [1-3]. It is basically a transmission line in which the conductors are driven by slabs of explosive initiated by plane-wave detonation systems. Because the entire area of each driver plate moves simultaneously, the rate-of-change of the generator inductance remains high up to the end of the run. In addition the plates may be made wide enough to carry large currents. We have used this type of generator in several applications requiring high output power [4-7]. The basic design is shown in Fig. 1.

It is important to be able to model explosive-driven generators in a general lumped-parameter circuit code. Such models are invaluable for quick feasibility calculations involving new applications and for optimizing parameters in experimental designs. Figure 2 shows a schematic representation of an explosive generator regarded as a circuit element.

The input switch usually closes when the generator starts its run and $L_g(t)$ starts changing. The output switch closes when the moving conductors finally short the generator output. During the generator run, the generator is represented by a decreasing inductance, $L_g(t)$, in series with a time-varying resistance, $R_g(t)$. This particular model is applicable only if the initial flux is generated by a current through the generator. If the initial flux arises from magnetic coupling to a coil or magnetic system, the model must be extended to include the time-varying coupling as well. The resistor, $R_g(t)$, is often used to account for the flux losses

from diffusion into the conductors and trapping near points of contact. However, for the plate generator we shall assume that $R_g \equiv 0$ and account for flux loss by leaving a small residual inductance in the generator at the end of the run.

The voltage across $L_g(t)$ is given by

$$V = I\, dL_g/dt + I_g\, dI/dt \quad . \tag{1}$$

I(t) is the current through the generator. Modeling the generator, then, amounts to finding convenient analytic expressions for $L_g(t)$ and dL_g/dt. We shall first express the plate separation, x(t), in the generator as a function of time and then express the generator inductance as a function of plate separation. That is,

$$L_g(t) = L_g[x(t)], \text{ and} \tag{2}$$

$$\frac{dL_g(t)}{dt} = \frac{\partial L_g}{\partial x}\frac{dx}{dt} \quad . \tag{3}$$

Note that the rate-of-change of the inductance is proportional to the driver plate velocity.

2. PLATE MOTION MODEL

Our first step is to find a simple expression for the behavior of the driver plates under the action of detonating explosives. The first arrival of the detonation front at the metal surface sends a shock through the driver plate. The interaction of the shock with the free surface at the interior of the generator sends a rarefaction fan back to the metal-explosive products interface. This rarefaction is reflected as a pressure wave. The process continues and the velocity of the plate builds up correspondingly. There are many one-dimensional codes that can calculate accurately the velocity and distance as a function of time. The difficulty is that we need a simple analytic model that gives the same results. The model need not be very accurate during the early part of the generator run where the change in the generator inductance is only a small part of the total circuit inductance. The critical portion is near the end of the generator run when the plates have traveled some distance.

We have chosen the following equation to represent the plate velocity since it demonstrates the proper asymptotic behavior:

$$v(t) = \frac{dx}{dt} = v_0 + v_1[1 - \exp(-t/\tau)] \quad . \tag{4}$$

$v(t)$ is the plate velocity during the generator run; v_0 represents the plate velocity at $t = 0+$, corresponding to but not necessarily equal to the free surface velocity at first shock arrival; v_1 is the additional velocity imparted to the plate by the later action of the explosive reaction pro-

ducts; and τ is the time constant that governs the build-up to the asymptotic velocity $v_0 + v_1$ and is related to the reverberation time of the shocks and rarefactions in the plate. The equation for the position, x(t), of the plate, obtained by integrating Eq. (4), is

$$x(t) = x_0 + (v_0 + v_1)t - v_1\tau[1 - \exp(-t/\tau)] \quad . \tag{5}$$

x_0 is the initial position of the plate. The velocity function is discontinuous, being equal to zero for $t < 0$ and rising abruptly to v_0 at $t = 0+$. The acceleration function corresponding to Eq. (4) is

$$a(t) = \frac{dv}{dt} = v_0\,\delta(t) + (v_1/\tau)\exp(-t/\tau) \quad . \tag{6}$$

$\delta(t)$ is the Dirac delta-function and is necessary to inject v_0 at $t = 0$ when the expression is integrated. For $t < 0$, $a(t) = 0$. A term proportional to I^2 may be added to Eq. (6) to account for the deceleration caused by magnetic pressure.

A variety of problems representative of the explosive and driver plate combinations we wanted to use were checked against PAD [8], a one-dimensional hydrodynamics code developed at Los Alamos by W. Fickett. Figure 3 shows a comparison of the velocity curves predicted by PAD and the analytic model. The system consisted of 7.62 cm of PBX 9404 with a 1.588-mm copper driver plate. The parameters of the analytic model were chosen to give the best fit to the x(t) curve at later times. The fit to the v(t) curve is good. The x(t) curve is not shown since the deviation is only 0.4 mm near the start and less than 0.02 mm near the end of the run.

The final test of the plate motion model is a comparison with experimental data. The most convenient measurement technique to use was the axially symmetric magnetic pickup [9] since it yields a signal proportional to the plate velocity. Several shots were fired using representative explosive-driver plate combinations. Figure 4 shows the comparison between the model and the experimental data [10]. The explosive was 5.08 cm of PBX 9404 and the driver plate 3.19 mm of 6061 aluminum. Again, the model parameters were adjusted to give a good fit to the x(t) curve at late times. The x(t) curve is not shown because the maximum deviation was only 0.1 mm. Similar results were obtained with the other shot data. We concluded that the analytic model gave an excellent representation of the plate motion.

3. INDUCTANCE MODEL

The final step in the modeling procedure is to relate the plate separation to the generator inductance. The task is not an easy one. Flash x-ray photographs of a driven plate from the side and end show that it looks like an oblong pincushion with a valley down each side. To add to the complication, the current density is not uniform over the plate. The time scale of the generator run is sufficiently short that the flux is excluded from the interior of the plate. The result is that the surface current density cannot be uniform and satisfy the boundary conditions.

Our approach is to take the simplest model that accounts for edge effects and the fact that the transmission plates may not be parallel. We make the following assumptions:

(1) The plates are plane rectangles;

(2) The current is confined to the surface, is uniform and directed along the length of the plate;

(3) Finite length and end effects may be neglected.

The formula usually associated with a parallel plate transmission line is

$$L_g = \mu_0 \ell \eta \quad . \tag{7}$$

L_g is the inductance in Henries; ℓ is the length in meters; η is the

separation/width; and $\mu_0 = 4\pi \times 10^{-7}$ H/m. This expression is accurate for $\eta << 1$. However, the initial η for most plate generators is close to one and the preceeding formula is inaccurate by a factor of two. Therefore, we must use a formula that takes into account the edge effects. It is a straightforward matter to perform the necessary integrations to obtain

$$L_g = \frac{\mu_0}{2\pi} \ell \, G(\eta) \quad , \tag{8}$$

where

$$G(\eta) = 4\eta \tan^{-1}(1/\eta) + \ell n(1 + \eta^2) - \eta^2 \ell n(1 + 1/\eta^2) \quad .$$

A graph of this function is given in [11]. We shall also need the derivative to calculate dL_g/dt.

$$\frac{dG}{d\eta} = 4 \tan^{-1}(1/\eta) - 2\eta \ell n(1 + 1/\eta^2) \quad . \tag{9}$$

These formulas provide us with a good estimate of the inductance of a parallel plate generator and its rate of change. Many applications, however, require a geometry in which the plates are tilted to form a trapezoidal or triangular cross-section. Varying the input separation while keeping the output separation constant allows control over the voltage waveform [3]. Consequently, we need the expressions for these cases.

Figure 5 illustrates the geometry involved in the trapezoidal configuration along with the key dimensions. One can obtain an estimate of the inductance by averaging the inductance per unit length over the projected length of the driver plates using the formula for the rectangular geometry. The integration gives

$$L_g = \frac{\mu_0}{2\pi} \frac{\ell}{\eta_0} [F(\eta) - F(\eta - \eta_0)] \quad , \tag{10}$$

where

$$\eta_0 = (x_0 - x_{10})/w \quad ,$$

$$\eta = x/w \quad , \text{ and}$$

$$F(\eta) = 2(\frac{2}{3} + \eta^2) \tan^{-1}(1/\eta) + 2 \tan^{-1}(\eta)$$

$$+ \eta \ln(1 + \eta^2) - \frac{1}{3} \eta^3 \ln(1 + 1/\eta^2) - \frac{2}{3} \eta \quad .$$

The quantity η_0 is a constant. x_{10} and x_0 are the initial plate separations at the input and output ends, respectively, and x is the plate separation at the output end as a function of time.

The formula for the triangle is quite similar:

$$L_g = \frac{\mu_0}{2\pi} \frac{\ell}{\eta} [F(\eta) - F(0)] \quad . \tag{11}$$

It should be noted that, since the length of the triangular generator is proportional to the separation distance, ℓ/η is proportional to w. The derivative of $F(\eta)$ is

$$\frac{dF}{d\eta} = G(\eta) \quad . \tag{12}$$

The values of the functions as $\eta \to 0$ are

$$F(0) = \frac{2}{3}\pi \quad ,$$

$$G(0) = 0 \quad , \text{ and}$$

$$\frac{dG(0)}{d\eta} = 2\pi \quad .$$

It was stated earlier that the driver plates do not move as plane rectangles but develop a lag at the edges as they run. We cannot tackle the real geometry within our restrictions, but we can allow some variation in w as the plates move. The simplest formulation is to take w_0 as the initial width of the plates, w_1 as a final "effective" width of the plates when the separation goes to zero and assume a linear variation with plate separation between the two values. w_1 should be regarded as an adjustable parameter and can be estimated from the end-on flash x-ray radiographs. Mathematically,

$$w(x) = w_1 + k_0 x \quad , \tag{13}$$

where

$$k_0 = \frac{w_0 - w_1}{x_0} \quad .$$

The derivative is

$$\frac{dw}{dt} = k_0 v \quad . \tag{14}$$

The length of the driver plates also varies during the generator run. The reason is that the end blocks are cut at an angle to the vertical in order to maintain good current contact with the driver plates. The relevant geometry is shown in Fig. 6. We can estimate this effect by assuming that the additional flux excluded by the protrusion at an end block is proportional to its cross-sectional area. Then, the effective length is

$$\ell = \ell_0 - k_1 x_0 + \frac{1}{2} k_1 x \quad \text{(rectangle)} \quad , \tag{15a}$$

$$\ell = \ell_0 - \frac{1}{2}(x_0 + x_{10}) + \frac{1}{2} k_1 x \quad \text{(trapezoid)} \quad , \tag{15b}$$

$$\ell = k_1 x \quad \text{(triangle)} \quad . \tag{15c}$$

Here, ℓ_0 is the projection of the initial plate length on the generator midplane. The constant k_1 is defined as follows.

$$k_1 = \frac{1}{2}(\tan\alpha + \tan\beta) \quad \text{for the rectangle and trapezoid,}$$

$$k_1 = \ell_0/x_0 - \frac{1}{4}\tan\beta \quad \text{for the triangle.}$$

The derivatives are

$$\frac{d\ell}{dt} = \frac{1}{2} k_1 v \quad \text{(rectangle and trapezoid)} , \tag{16a}$$

$$\frac{d\ell}{dt} = k_1 v \quad \text{(triangle)} . \tag{16b}$$

As the final touch-up to the calculations, we would like to estimate the residual inductance left in the generator when the output is finally shorted. The simplest assumption, again, is an inductance that grows in a linear fashion as the separation decreases. Since the field increases with time, the diffused flux does not vary as $\sqrt{t}$. The formula is

$$L_e(x) = L_f (1 - x/x_0) . \tag{17}$$

L_f is the final inductance left when generator action is complete. We

treat it as an adjustable parameter that can be estimated from more detailed flux diffusion calculations. The derivative is

$$\frac{dL_e}{dt} = -\frac{L_f}{x_0} v \quad . \tag{18}$$

We still need the explicit form of dL_g/dt in order to complete the computation. Noting that

$$\frac{dn}{dt} = \frac{v}{w} (1 - k_0 n) \quad ,$$

we have

$$\frac{dL_g}{dt} = v(t)\left\{\frac{\mu_0}{2\pi}\left[\frac{1}{2} k_1 G(n) + \frac{\ell}{w} (1 - k_0 n) \frac{dG(n)}{dn}\right] - \frac{L_f}{x_{20}}\right\}$$

for the rectangle; (19)

$$\frac{dL_g}{dt} = v(t)\left\{\frac{\mu_0/2\pi}{n_0} \cdot \frac{1}{2} k_1 [F(n) - F(n - n_0)]\right.$$

$$\left. + \frac{\ell}{w} (1 - k_0 n)[G(n) - G(n - n_0)] - \frac{L_f}{x_0}\right\}$$

for the trapezoid; and (20)

$$\frac{dL_g}{dt} = v(t) \left\{\frac{\mu_0}{2\pi\eta} \left\{\left[k_1 - \frac{\ell}{w\eta}(1 - k_0\eta)\right]\left[F(\eta) - F(0)\right] + \ell G(\eta)\right\} - \frac{L_f}{x_0}\right\}$$

for the triangle . (21)

The computational procedure starts with calculating x(t) and v(t) from Eqs. (5) and (4). The w(x), $\ell(x)$ and $L_e(x)$ are calculated from Eqs. (13), (15) and (17). $L_g(x)$ is obtained from Eqs. (8), (10) or (11) and dL_g/dt from Eqs. (19), (20) or (21), depending on the geometry. It is worth noting that neither L_g nor dL_g/dt are discontinuous in the transition from a trapezoidal to a triangular shape. Also, since x(t) now represents plate separation rather than distance traveled, v_0 and v_1 are negative and twice the values for a single plate.

4. COMPARISON WITH DATA

The critical test of any model is comparison with the data. In the present instance, we would like to measure both L_g and dL_g/dt in actual generator shots. The experiments must be designed to be sensitive to these particular quantities with a minimum of interference from other, possibly time-varying, effects. The best method we have found is to fire the generators into a very low inductance load. The current should be kept low enough to prevent appreciable motion of the output and load conductors before generator action is complete. Taking L_ℓ as the load inductance and lumping any losses in with the generator inductance, we have

$$\frac{I(t)}{I_0} = \frac{L_g(0) + L_\ell}{L_g(t) + L_\ell} \quad , \text{ and} \tag{22}$$

$$\frac{1}{I}\frac{dI}{dt} = \frac{dL_g/dt}{L_g(t) + L_\ell} \quad . \tag{23}$$

Here, I_0 is the initial current in the generator and load. If $L_g(0)$ and L_ℓ are known accurately, then $I(t)/I_0$ gives $L_g(t)$ and $\dot{I}/I$ gives dL_g/dt. It is evident from the equations that making L_ℓ as small as possible permits the best measurements of L_g and dL_g/dt near the end of the run.

We present here a comparison of the model calculations with the results of two experiments. The parameters were the same for both except for the input plate separation. The driver plates were 3.19-mm aluminum driven by 1.08 cm of PBX 9404 -- the same system modeled in Fig. 4. The

initial length was 525 mm, the initial width 159 mm and the final width 114 mm. The output separation was 127 mm. The load was a one-turn coil just large enough to admit a Rogowski loop without close contact at the corners. The load inductance was 2.6 nH. The final end inductance was taken to be 9 nH. The generator action was assumed to be over when the plate separation at the output reached 1 mm, corresponding to the insulation thickness in the output slot.

The first generator had an input separation of 101.6 mm, corresponding to a trapezoidal geometry. The input separation of the second generator was about 0.5 mm, corresponding to a triangular geometry. The inductance versus time curves are compared in Fig. 7.

The agreement with the experimental results is excellent. A more demanding comparison, however, is between the derivative curves. Figure 8 shows dL_g/dt versus time. It is evident that the lumped-parameter model gives a reasonable approximation to the actual behavior.

5. DISCUSSION

The analytic generator model has shown a pleasing similarity to real generator behavior where we have tested it. It has proven to be quite useful in judging the applicability of the plate generator to a number of proposed plasma experiments. We also employ the model extensively in estimating the timing and recording channel coverage for many experiments. Future work is aimed at taking into account the effects of nonlinear flux diffusion and magnetic pressure.

ACKNOWLEDGEMENTS

The authors thank J. N. Fritz and J. A. Morgan for the experimental data on plate motion.

REFERENCES

[1] C. M. FOWLER, R. S. CAIRD, W. B. GARN, D. B. THOMSON, in High Magnetic Fields, edited by H. Kolm, B. Lax, F. Bitter and R. Mills, The M.I.T. Press, Cambridge, Massachusetts (1962), Ch. 25, 275.

[2] R. S. CAIRD, D. J. ERICKSON, W. B. GARN, C. M. FOWLER, in Proceedings IEEE International Pulsed Power Conference, Institute of Electrical and Electronic Engineers, New York (1976), Paper III D-3.

[3] R. S. CAIRD, C. M. FOWLER, D. J. ERICKSON, B. L. FREEMAN, W. B. GARN, in Energy Storage, Compression and Switching, Vol. 2, Plenum, New York (1983) 1.

[4] C. M. FOWLER, R. S. CAIRD, D. J. ERICKSON, B. L. FREEMAN, D. B. THOMSON, W. B. GARN, in Energy Storage, Compression and Switching, Vol. 2, Plenum, New York (1983) 19.

[5] B. L. FREEMAN, R. S. CAIRD, D. J. ERICKSON, C. M. FOWLER, W. B. GARN, ET AL., Plasma Focus Experiments Powered by Explosive Generators, paper in this conference.

[6] J. H. GOFORTH, R. S. CAIRD, R. F. BENJAMIN, D. J. ERICKSON, C. M. FOWLER, B. L. FREEMAN, Fast Explosive-Driven Opening Switches Carrying High Linear Current Densities, paper in this conference.

[7] D. J. ERICKSON, R. S. CAIRD, C. M. FOWLER, B. L. FREEMAN, W. B. GARN J. H. GOFORTH, A Megavolt Pulse Transformer Powered by a Fast Plate Generator, paper in this conference.

[8] W. FICKETT, PAD, a One-Dimensional Lagrangian Hydrocode, Los Alamos National Laboratory Report, LA-5910-MS (1975).

[9] J. N. FRITZ, J. A. MORGAN, Rev. Sci. Instr. 44, 215 (1973).

[10] J. N. FRITZ, J. A. MORGAN, Los Alamos Scientific Laboratory, private communication (22 Feb 1977).

[11] H. KNOEPFEL, Pulsed High Magnetic Fields, North Holland Publishing Co. (1970) 323.

FIGURE CAPTIONS

Figure 1. Drawing of a plate generator. The slabs of explosive are initiated by a plane-wave system.

Figure 2. Schematic of an explosive-driven generator as a lumped-parameter element. The input switch closes when the generator starts its run; the output switch closes when the generator completes its run.

Figure 3. Comparison of PAD calculations with the analytic model for a 7.62-cm slab of PBX-9404 and a 1.588-mm copper driver plate.

Figure 4. Comparison of shot data with the analytic model for a 5.08-cm slab of PBX-9404 and a 3.19-mm aluminum driver plate.

Figure 5. Trapezoidal generator shape used for inductance calculations.

Figure 6. Shape of the input and output blocks for a plate generator. The reentrant geometry is necessary to maintain good current contact.

Figure 7. Comparison of the generator inductance predicted by the model with experimental results. The parameters are given in the text.

Figure 8. Comparison of dL_g/dt predicted by the model with experimental results. The parameters are given in the text.

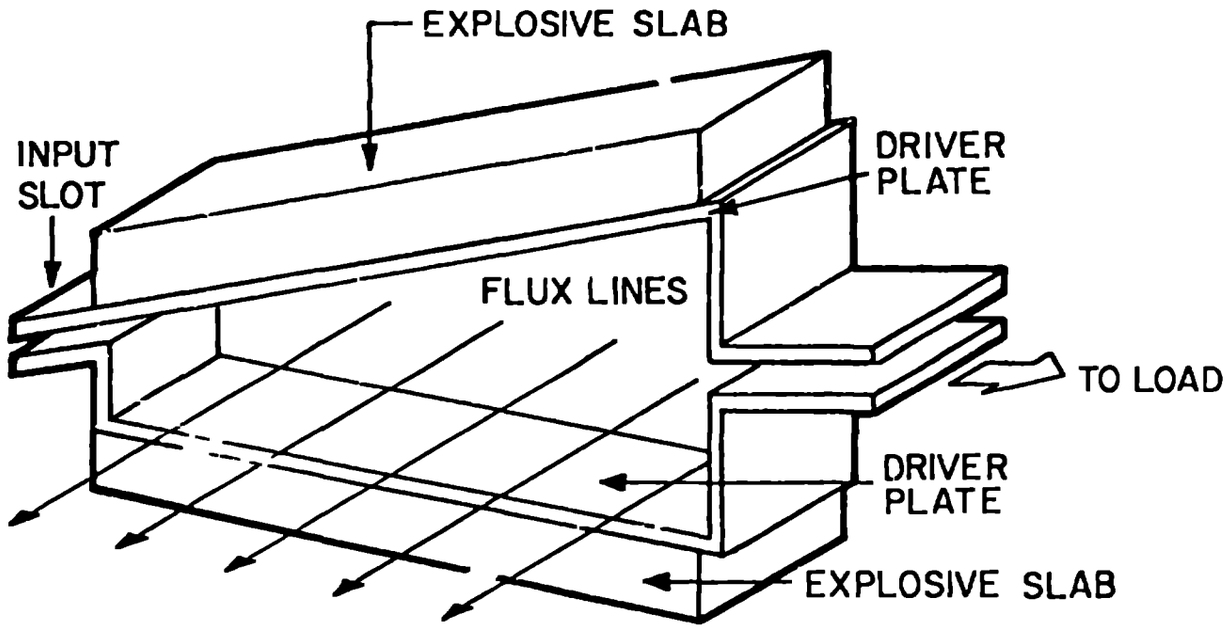

EXPLOSIVE SLAB
INPUT SLOT
DRIVER PLATE
FLUX LINES
TO LOAD
DRIVER PLATE
EXPLOSIVE SLAB

Fig. 1

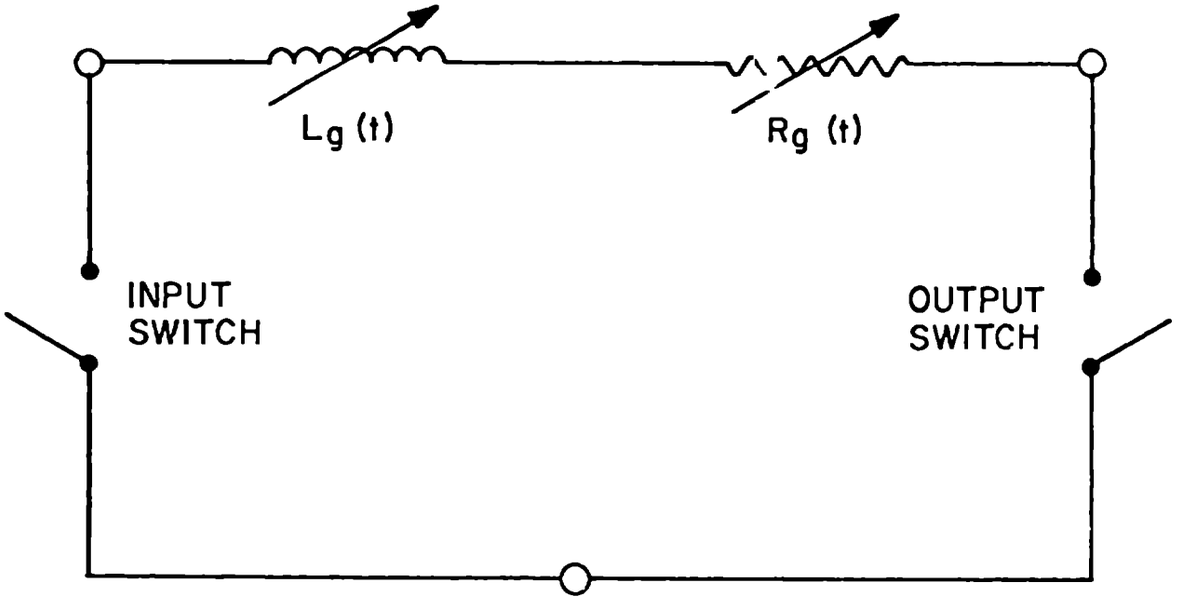


Fig. 2

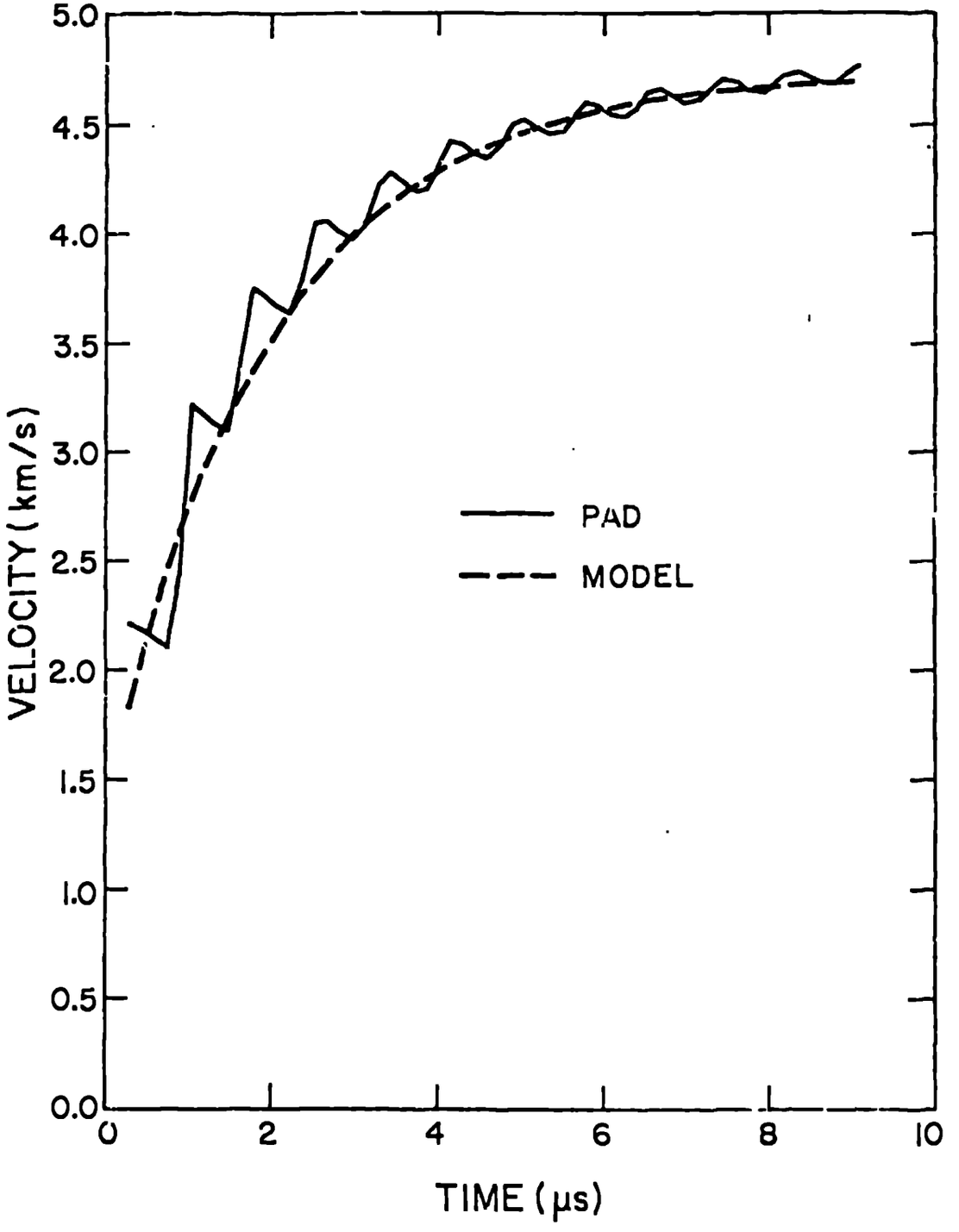

5.0
4.5
4.0
3.5
3.0
2.5
2.0
1.5
1.0
0.5
0.0
VELOCITY (km/s)
0
2
4
6
8
10
TIME (μs)
PAD
MODEL

Fig. 3

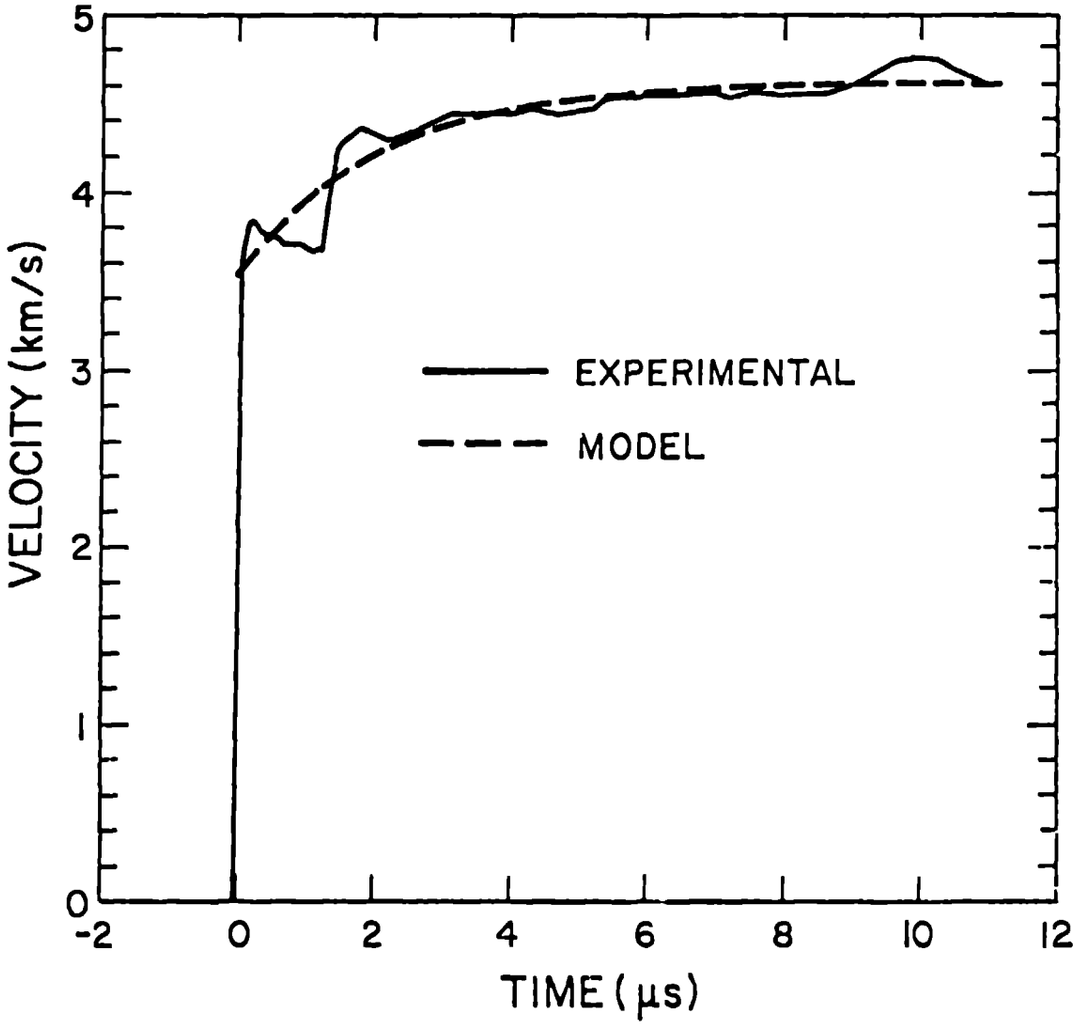

VELOCITY (km/s)
TIME (μs)
EXPERIMENTAL
MODEL
0
1
2
3
4
5
-2
0
2
4
6
8
10
12

Fig. 4

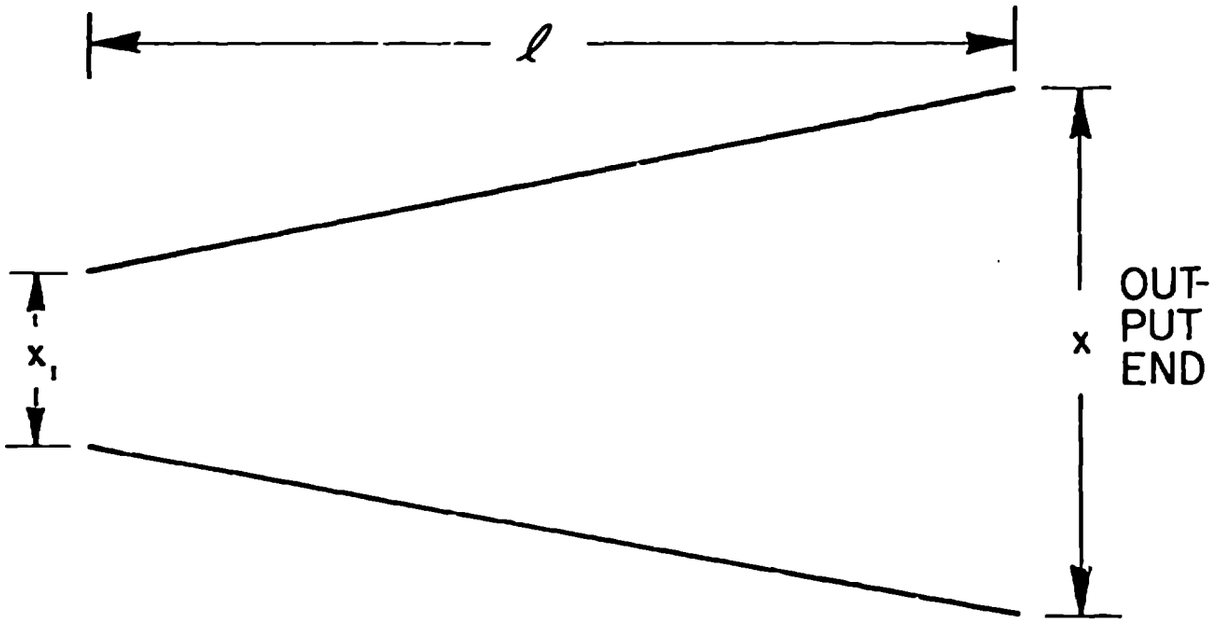


Fig. 5

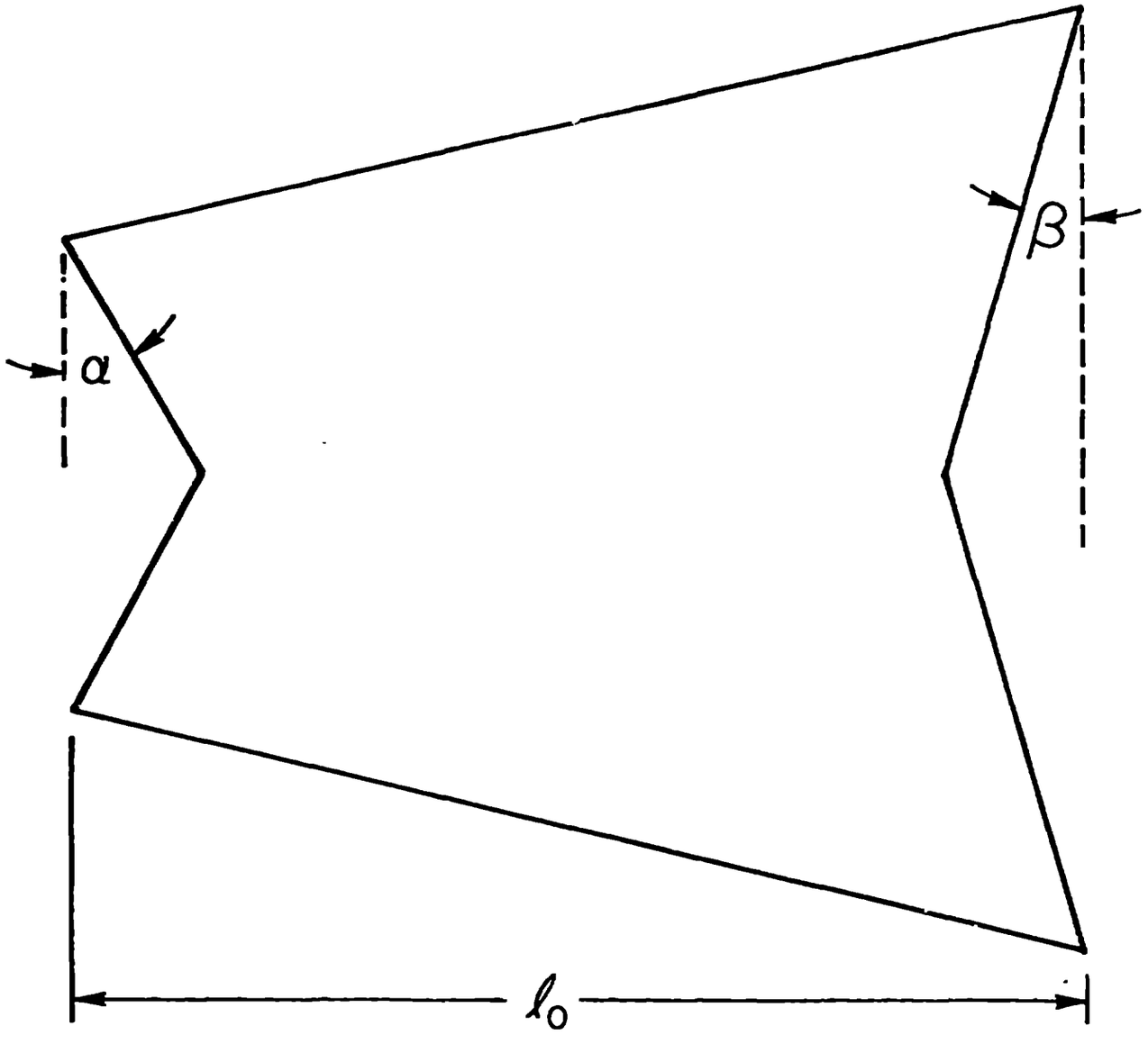


Fig. 6

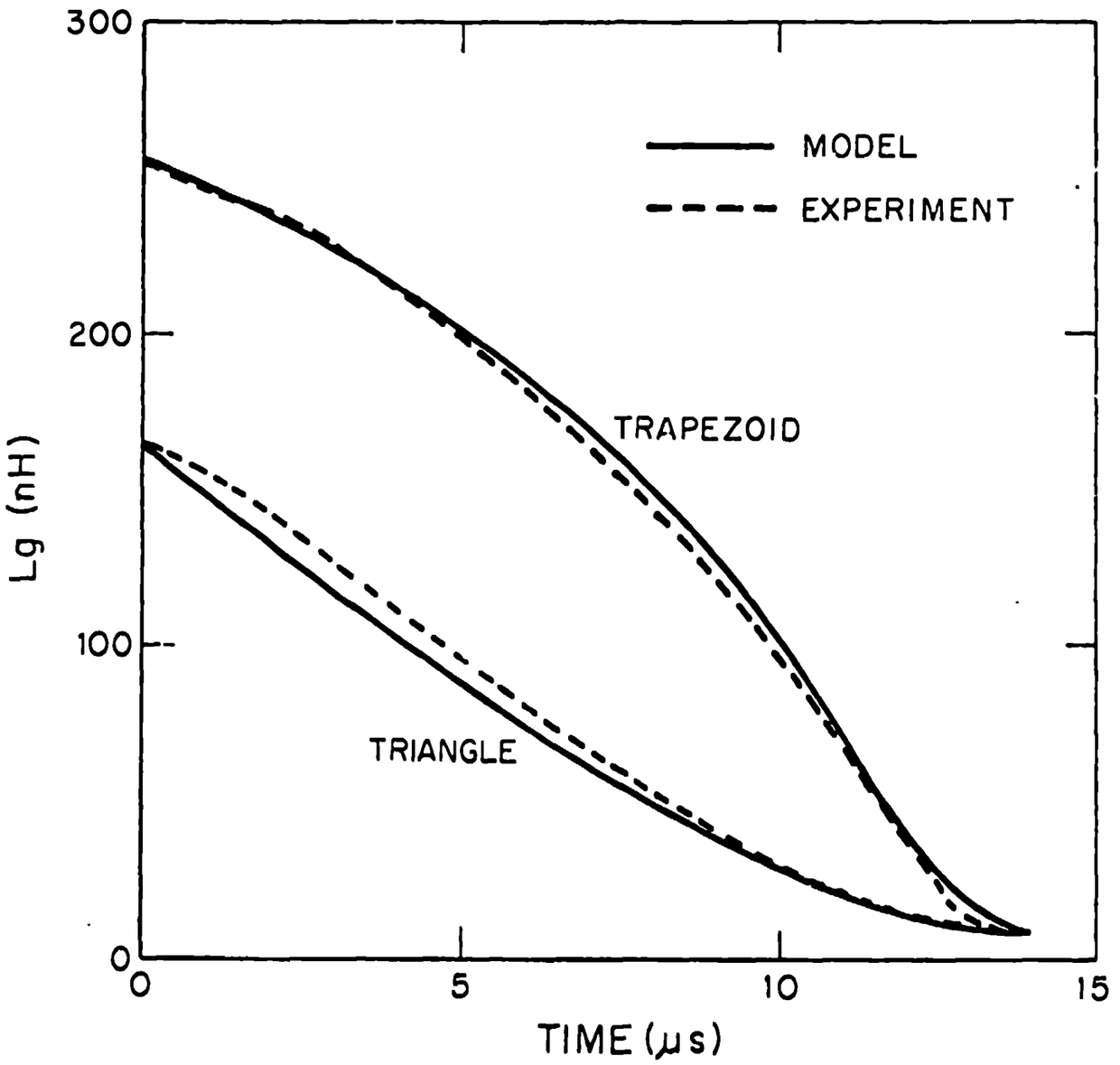

300
200
100
0
Lg (nH)
MODEL
EXPERIMENT
TRAPEZOID
TRIANGLE
0
5
10
15
TIME (μs)

Fig. 7

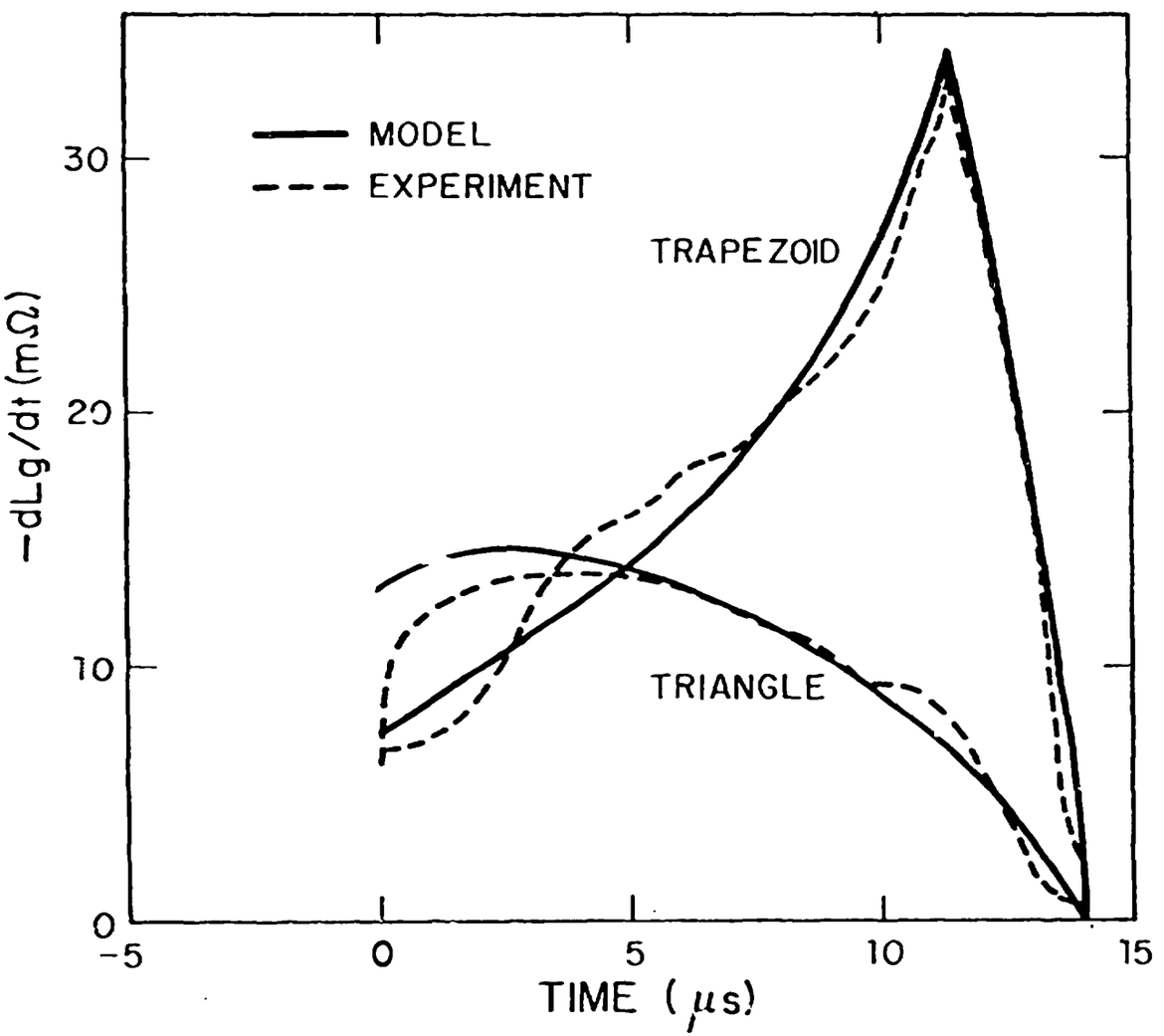

MODEL
EXPERIMENT
TRAPEZOID
TRIANGLE
-dLg/dt (mΩ)
30
20
10
0
-5
0
5
10
15
TIME (μs)

Fig. 8